

Stress analysis of selective epitaxial growth of GaN

Q. K. K. Liu^{a)}

Bereich Theoretische Physik, Hahn-Meitner-Institut, Glienicke Str. 100, D-14109 Berlin, Germany

A. Hoffmann, H. Siegle, A. Kaschner, and C. Thomsen

Institut für Festkörperphysik, Technische Universität Berlin, D-10623 Berlin, Germany

J. Christen and F. Bertram

Institut für Experimentelle Physik, Otto-von-Guericke-Universität Magdeburg,

D-39016 Magdeburg, Germany

(Received 3 February 1999; accepted for publication 29 March 1999)

Stress distributions in selectively overgrown self-organized GaN hexagonal pyramids have been analyzed by continuum elasticity theory. This has been carried out using the values for the moduli of elasticity found in the literature and an effective lattice mismatch between the GaN and the substrate that was determined from the Raman shift of the GaN buffer layer. The results of compressive stress in the buffer layer, tensile stress on the lower half of the pyramids' facet surface, and full relaxation for approximately the upper 2/3 of the pyramids are in satisfactory agreement with the experimental observations that were deduced from cathodoluminescence microscopy and micro-Raman spectroscopy. © 1999 American Institute of Physics. [S0003-6951(99)00121-7]

Wideband-gap group III nitrides are being studied extensively for their application potential in optoelectronic and microelectronic devices.¹ The selective growth technique plays a key role in this field,² along with the control of strain in low-dimensional heterostructures based on GaN. In order to fabricate micro- and nanostructures, dry etching is frequently employed,^{3,4} often resulting in severe damage and contamination of the surface. Selective overgrowth, which has been seen to facilitate three-dimensional (3D) control of microstructures such as quantum wires and quantum dots, can overcome these problems. Reduction in dislocation density has been observed in selectively overgrown GaN pyramids,⁵ and laser action has been observed in GaN pyramids selectively overgrown on Si(111).⁶

The purpose of the present study is to use analysis based on continuum elasticity theory to provide support for the experimental optical characterization of selectively overgrown self-organized GaN pyramids.

Using metalorganic vapor phase epitaxy (MOVPE), selective growth of GaN and AlGaN on linearly patterned GaN(0001)/sapphire substrate⁷ and the growth of three-dimensionally controlled structures have been reported.^{8,9} For the sample in our present discussion, a 2- μm -thick GaN(0001) was first grown on a sapphire substrate [on axis $\alpha\text{-Al}_2\text{O}_3$ (11 $\bar{2}$ 0)] using an AlN buffer layer. A 50–60 nm thick SiO₂ mask was patterned by photolithography and subsequently etched to form hexagonal windows. The pattern consisted of three periodic triangular lattices of hexagons of 5 μm width and lateral separations of 10, 20, and 40 μm , respectively. Epitaxial GaN was selectively grown on top, using hydride vapor phase epitaxy (HVPE), creating the periodic arrays of hexagonally shaped pyramids covered by the six {1 $\bar{1}$ 01} pyramidal facets. No GaN was deposited on the SiO₂ mask.

The microscopic optical characterization using cathodoluminescence (CL) microscopy and micro-Raman spectroscopy has been described elsewhere.¹⁰ The CL spectrum $I(x_i, y_i, \lambda)$ was expressed as a function of position (x_i, y_i) on the scanning surface of the sample and the emission wavelength λ , or as a line scan $I(s, \lambda)$, where s is the distance along a given path. For micro-Raman spectroscopy the spatial resolution was better than 1 μm and Raman shifts smaller than 0.1 cm^{-1} could be detected.¹¹

The results of the low temperature (5° K) CL microscopy is exemplified in the line scan shown in Fig. 1. The photon from the decay of the neutral-donor-exciton complex (D^0, X) in relaxed GaN has a wavelength $\lambda=357.1$ nm (3.471 eV).¹¹ At the base of the pyramid ($s=0$), a strongly redshifted luminescence ($\lambda>361$ nm, i.e., $E<3.433$ eV) is observed. Within 3 μm from the base of the nearly 10 μm length of the pyramid facet, λ decreases to the relaxed value of 357.1 nm. A narrow blueshifted luminescence peak at $\lambda=355.0$ nm (3.492 eV), originating from the 2 μm GaN buffer layer, is also observed.

The micro-Raman measurements at room temperature (RT) that are of direct relevance to our analysis are shown in Fig. 2. The upper part of the pyramid is observed to be fully relaxed, whereas the 2 μm buffer layer showed a Raman shift of 4 cm^{-1} for the E_2 (high) phonon mode, from which it can be deduced that the stress tensor elements $\sigma_{xx} = \sigma_{yy} = -0.95$ GPa.¹⁰ This is in excellent agreement with the CL spectroscopy results.

The stress distributions inside the 2 μm GaN buffer layer and the pyramids have been investigated theoretically using elasticity theory simulated by the finite-element method (FEM).¹² The ingredients for elasticity theory are the mismatch α between GaN and the substrate and a set of moduli of elasticity. In the case of coherent epitaxial growth, α would have been given by the difference in the lattice constants. From the size of the sample and the growth process, we expect defects, impurities and dislocations to be

^{a)}Electronic mail: liu@hmi.de

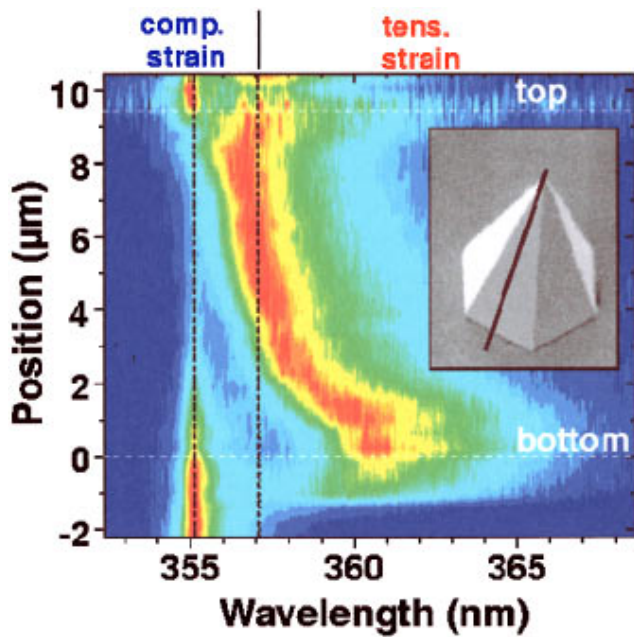


FIG. 1. CL spectrum line scan $I(s, \lambda)$ at $T=5^\circ \text{K}$ along a $\{1\bar{1}01\}$ facet of a pyramid. The white dashed lines mark the top and bottom of the GaN pyramid. The spectral positions of (D^0, X) emission from the compressively stressed $2 \mu\text{m}$ GaN layer (355 nm) and the fully relaxed GaN (357.1 nm) are marked by the vertical dotted lines.

present that would introduce large uncertainties into the theoretical values for α and the moduli of elasticity. In spite of this, our measurements seem to reflect a strong remnant of the epitaxial character of the material. We were therefore encouraged to incorporate these uncertainties into an effective mismatch parameter α_{eff} between GaN and the sapphire substrate, and continue to use the experimental values for the moduli of elasticity from the literature. The value of α_{eff} was adjusted to produce the stress tensor elements σ_{xx} and σ_{yy} deduced for the $2 \mu\text{m}$ GaN layer.

Moduli of elasticity for stress-free hexagonal GaN from various authors have been tabulated in Ref. 13. Moreover, the stiffness matrix elements for the hexagonal GaN have been approximated by Young's moduli and Poisson ratios using Voigt averaging, i.e., moduli of elasticity for isotropic materials. Our simulations showed that there was no qualita-

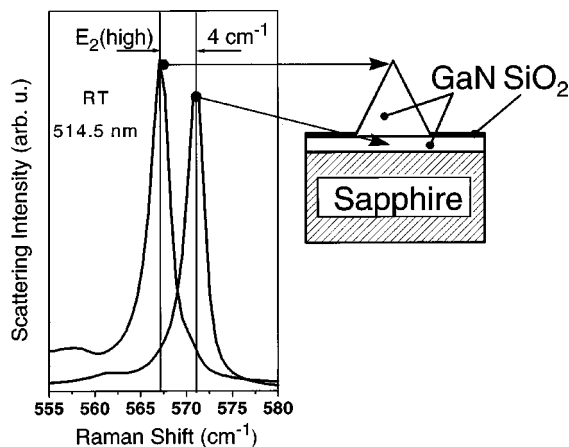


FIG. 2. Raman depth profile at RT. The solid curve represents a spectrum taken from the peak of the pyramid. The spectrum from the $2 \mu\text{m}$ GaN buffer layer is shown as a dashed curve.

TABLE I. The experimental moduli of elasticity of GaN.

c_{11} [GPa]	c_{12} [GPa]	c_{13} [GPa]	c_{33} [GPa]	c_{44} [GPa]
396	144	64	476	91

tive difference in the stress distributions resulting from different sets of moduli of elasticity, hexagonal or isotropic. To be specific, we have used for our present analysis the set from Ref. 14, tabulated in Table I. By setting $\alpha_{\text{eff}} = -0.2\%$ in the x - and y -directions, respectively, we have produced for a uniform biaxially stressed GaN film the diagonal stress tensor elements $\sigma_{xx} = \sigma_{yy} = -0.95 \text{ GPa}$ and $\sigma_{zz} = 0 \text{ GPa}$, i.e., our sample GaN film has to be compressed in the x and y directions by 0.2% , respectively. As further simulations demonstrated, σ_{xx} and σ_{yy} remained the same in large parts of the GaN buffer layer even in the presence of pyramids. For the results we report in this investigation, the lateral separation of the pyramids was $10 \mu\text{m}$, the width of the hexagon $6.66 \mu\text{m}$, and the height of the pyramid $10 \mu\text{m}$. Due to rotation and mirror symmetries of the hexagon, simulation of only $1/12$ of the materials was necessary.

The experimental results can be discussed in terms of the mean stress from FEM defined as $(\sigma_{xx} + \sigma_{yy} + \sigma_{zz})/3$ shown in Fig. 3. This mean stress has its minimum value of -1.5 GPa in a small volume at the junctions of the facets and the buffer layer. However, for the rest of the buffer layer, we have $\sigma_{xx} \approx \sigma_{yy} \approx -1 \text{ GPa}$ nearly everywhere and their absolute values dominate over all the other stress tensor elements by an order of magnitude. Therefore, the negative sign of the mean stress in the buffer layer in Fig. 3 signifies a biaxial compressive stress. In an area on the lower half of the facet surface of the pyramid, we have $\sigma_{zz} \approx 0.25 \text{ GPa}$ and its absolute value dominates over all the other stress tensor elements by a factor of 5 to 6. Therefore, the positive sign of the mean stress on the facet surface of the pyramid in Fig. 3

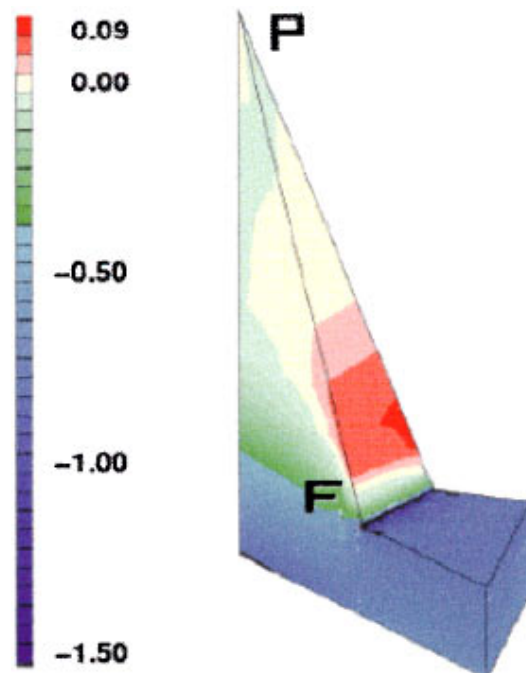


FIG. 3. Mean stress distribution (GPa) inside the pyramid and in the GaN layer.

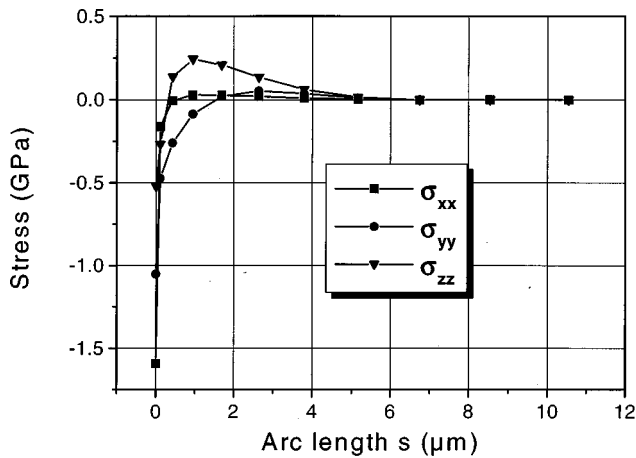


FIG. 4. Components of the stress tensor on mid facet of the pyramid.

signifies a tensile stress in the z direction. These conclusions are confirmed by diagonalizing the respective stress tensors to obtain the corresponding principle stresses. For the materials further towards the peak of the pyramid, all the stress tensor elements become vanishingly small, indicating full relaxation. The entire picture agrees with the results of the CL of Fig. 1, i.e., blueshifted CL from the compressively stressed GaN buffer layer, redshifted CL from the tensile stressed facet surface near the base of the pyramid, with the top of the pyramid fully relaxed. The line indicated in the inset of Fig. 1 corresponds to the foot-to-peak line FP in Fig. 3. In Fig. 4 we display the theoretical results for the elements σ_{xx} , σ_{yy} , and σ_{zz} , evaluated along the line FP that spans a distance of $10.5 \mu\text{m}$. The results confirm the experimental observations that the stress-free volume extends nearly $2/3$ of the way down from the top of the pyramid.

It is not reasonable to expect that a set of moduli of elasticity and an effective lattice mismatch parameter are sufficient to describe in quantitative detail the mechanical response of our GaN sample of μm in dimension, because the latter must contain defects, impurities and a myriad dislocations. However, it is also understandable, without recourse to the details of the moduli of elasticity, that, if a lattice mismatch causes σ_{xx} and σ_{yy} to be negative in the buffer layer, the material in the pyramid immediately above this layer will also be similarly stressed. As one moves away from the foot

of the pyramid towards the peak, the materials search out a path to relax the deformation energy. The relaxation is comparatively less restrained in the z direction than in the x and y directions. This gives rise to the possibility of σ_{zz} becoming positive and larger than σ_{xx} and σ_{yy} , as witnessed in Fig. 4. These features have also been seen in an analysis of self-organized coherent InP islands on GaP.¹⁵ In this case, the lattice mismatch is approximately -7% , and the region of positive σ_{zz} is found nearer to the peak of the island.

In conclusion, the overall picture of the stress distributions of selectively overgrown self-organized GaN hexagonal pyramids on a lattice-mismatched substrate investigated by CL microscopy and micro-Raman spectroscopy has been confirmed by analysis based on continuum elasticity theory. The stress distributions are characterized by compressive stress in the buffer layer, tensile stress on the pyramid facets near the base, and full relaxation in the mid to upper portion of the pyramid.

- ¹For a review, see S. Nakamura and G. Fasol, *The Blue Laser Diode* (Springer, Heidelberg, 1997).
- ²S. Nakamura, M. Senoh, S. Nagahama, N. Iwasa, T. Yamada, T. Matsushita, H. Kiyoku, Y. Sugimoto, T. Kozaki, H. Umemoto, M. Sano, and K. Chocho, *Appl. Phys. Lett.* **72**, 2014 (1998).
- ³H. Lee, D. B. Oberman, and J. S. Harris, Jr., *Appl. Phys. Lett.* **67**, 1754 (1995).
- ⁴R. T. Leonard and S. M. Bedair, *Appl. Phys. Lett.* **68**, 794 (1996).
- ⁵T. S. Zheleva, O.-H. Nam, M. D. Bremser, and R. F. Davis, *Appl. Phys. Lett.* **71**, 2472 (1997).
- ⁶S. Bidnyk, B. D. Little, Y. H. Cho, J. Krasinski, J. J. Song, W. Yang, and S. A. McPherson, *Appl. Phys. Lett.* **73**, 2242 (1998).
- ⁷Y. Kato, S. Kitamura, K. Hiramatsu, and N. Sawaki, *J. Cryst. Growth* **144**, 133 (1994).
- ⁸S. Kitamura, K. Hiramatsu, and N. Sawaki, *Jpn. J. Appl. Phys., Part 2* **34**, L1184 (1995).
- ⁹K. Hiramatsu, S. Kitamura, and N. Sawaki, *Mater. Res. Soc. Symp. Proc.* **395**, 267 (1996).
- ¹⁰F. Bertram, J. Christen, M. Schmidt, K. Hiramatsu, S. Kitamura, and N. Sawaki, *Physica E* **2**, 552 (1998).
- ¹¹H. Siegle, A. Hoffmann, L. Eckey, C. Christen, F. Bertram, D. Schmidt, and K. Hiramatsu, *Appl. Phys. Lett.* **71**, 2490 (1997).
- ¹²MARC Analysis Research Corporation, Palo Alto, CA 94306, *User's Guide* 1996.
- ¹³C. Kisielowski, J. Krueger, S. Ruvimov, T. Suski, J. W. Ager, E. Jones, Z. Lilienthal-Weber, M. Rubin, E. K. Weber, M. D. Bremser, and R. F. Davos, *Phys. Rev. B* **54**, 17745 (1996).
- ¹⁴S. Nakamura, M. Senoh, N. Iwasa, S. Nagahama, T. Yamada, T. Matsushita, H. Kiyoku, and Y. Sugimoto, *Jpn. J. Appl. Phys., Part 2* **35**, L217 (1996).
- ¹⁵Q. K. K. Liu, N. Moll, M. Scheffler, and E. Pehlke (unpublished).